https://doi.org/10.48048/tis.2025.9395

Protective Effects of Syringaresinol against UVB-Induced Human Dermal Fibroblast Senescence and Apoptosis

Nakuntwalai Wisidsri[1,*], Chaisak Chansriniyom[2,3] and Wacharee Limpanasitikul[4]

[1]Interdisciplinary Pharmacology Program, Graduate School, Chulalongkorn University, Bangkok 10330, Thailand
[2]Department of Pharmacognosy and Pharmaceutical Botany, Faculty of Pharmaceutical Sciences, Chulalongkorn University, Bangkok 10330, Thailand
[3]Center of Excellence in Natural Products and Nanoparticles (NP2), Chulalongkorn University, Bangkok 10330, Thailand
[4]Department of Pharmacology, Faculty of Medicine, Chulalongkorn University, Bangkok 10330, Thailand

([*]Corresponding author's e-mail: nakuntwalai_w@rmutt.ac.th)

Received: 26 November 2024, Revised: 6 January 2025, Accepted: 13 January 2025, Published: 20 February 2025

Abstract

UV radiation can cause skin photoaging by damaging DNA and generating excess intracellular ROS in skin cells. This study aimed to evaluate the protective effects of syringaresinol (Syr) isolated from *Carallia brachiata* on UVB-induced skin cell damage. Syr demonstrated potent antioxidant activity, IC_{50} 16.90 ± 0.89 μM, by DPPH assay. To evaluate the protective effect of Syr, human dermal fibroblasts, BJ cells, were pretreated with Syr, at noncytotoxic concentrations (3 - 30 μM), for 24 h before UVB irradiation. Syr increased cell survival and the levels of antioxidant enzymes, including superoxide dismutase (SOD), catalase (CAT), and heme oxygenase-1 (HO-1) of the irradiated cells. It also increased the level of nuclear Nrf-2, an important transcription factor for antioxidant gene expression. Syr suppressed UVB-induced ROS production. It attenuated UVB-induced cellular senescence by decreasing the number of β-galactosidase (β-gal) positive cells, suppressing p21, and reducing senescence-associated secretory phenotype (SASP) including levels of pro-inflammatory cytokines and matrix metalloproteinases (MMP1, MMP3), and increasing the level of collagen-1A1 (COL-1A1). Syr prevented UVB-induced DNA damage by decreasing cyclobutane pyrimidine dimer (CPD) photoproducts. Syr also suppressed UVB-induced apoptosis of BJ cells by decreasing the levels of active caspase 3, cleaved poly (ADP-ribose) polymerase (PARP). Syr remarkably inhibited the phosphorylation of extracellular signal-regulated kinase (ERK), c-Jun N-terminal kinase (JNK), and p38 mitogen-activated protein kinase (p38) proteins of the mitogen-activated protein kinase (MAPK) signaling pathway. It also inhibited the activation of nuclear factor kappa B (NF-κB). The results in this study suggest that Syr prevents UVB-induced dermal fibroblast damage, possibly via its antioxidant activity through down-regulating MAPK signaling and NF-κB activation. The protective effects of Syr lead to suppression of ROS production, DNA damage, senescence, and apoptosis of the UVB-irradiated cells.

Keywords: Syringaresinol, UVB, Human dermal fibroblasts, Antioxidant system, Cellular senescence, Apoptosis, Photoaging

Introduction

The skin is the body's outermost layer and is directly exposed to solar UV radiation, a significant environmental threat [1]. This exposure can lead to various skin damage, including erythema, edema, sunburn, keratinocyte hyperplasia, dryness, photoaging, and even skin cancer [2]. Among the types of UV radiation that reach the Earth's surface, UVB (280 - 320 nm) poses a greater risk to the skin than UVA (320 - 400 nm) [3].

UVB radiation is well-known to induce cellular oxidative stress by causing the overproduction of reactive oxygen species (ROS), which damages

intracellular proteins, lipids, RNA, and DNA [4]. As a highly energetic photon, UVB directly harms DNA by forming DNA lesions known as photoproducts [5]. The primary types of these lesions are cyclobutane pyrimidine dimers (CPDs) and pyrimidine (6-4) pyrimidone photoproducts (6-4PPs). If this DNA damage remains unrepaired, it can lead to cell cycle arrest, cellular senescence, apoptosis, or even carcinogenesis [6-7]. UVB-induced ROS and DNA damage are involved in activating main signaling pathways, including MAPKs and NF-κβ activation. Activation of these pathways contributes to cell cycle arrest and cellular senescence [8-10]. The senescent cells undergo permanent cell cycle arrest and exhibit a senescence-associated secretory phenotype (SASP) characterized by releasing pro-inflammatory cytokines, growth factors, and proteases [11-13].

Skin cells depend on their intracellular antioxidant systems to counteract UVB-induced ROS overproduction and maintain redox balance. Endogenous antioxidants such as SOD, CAT, and glutathione peroxidase (GPx) are critical for neutralizing harmful reactive molecules, including superoxide anions ($^{\bullet}O_{2-}$) and hydrogen peroxide (H_2O_2), by converting them into harmless substances like oxygen (O_2) and water (H_2O) [8]. The regulation of these antioxidants is primarily governed by the nuclear factor erythroid 2-related factor 2 (Nrf2). ROS stimulates the release of Nrf2 from its cytosolic inhibitor, Kelch-like ECH-associated protein 1 (Keap1). Once dislocated, Nrf2 is translocated to the nucleus and binds to antioxidant response elements (AREs) in the promoter regions of antioxidant genes, enhancing their expression to combat oxidative stress [10,14]. Excessive ROS levels can disrupt redox balance, leading to oxidative modifications of Nrf2 or its regulators. This impairs the ability of Nrf2 to activate antioxidant defenses, worsening cellular damage and oxidative stress-related conditions [15].

Syringaresinol (Syr) is a plant-derived lignan found in several food and medicinal plants, such as *Panax ginseng* [16], *Acanthopanax senticosus*, *Prunus mume* [17], *Magnolia thailandica* [18], *Rubia philippinensis* [19], *Ormosia hosiei* [20], and *Carallia brachiata* [21]. This compound exhibits many pharmacological activities and beneficial effects on human health. These include antioxidant [22], anti-tumor [23], anti-inflammatory [24-26], and cytoprotective effects [27,28]. The antioxidant and anti-inflammatory activities of Syr have been reported in several studies to protect or attenuate age-related skin atrophy [29], hypoxia-induced cardiomyocyte injury [26], diabetic nephropathy [22], and inflammation in sepsis-induced cardiac dysfunction [27]. These activities are mediated by up-regulating antioxidant enzymes, suppressing ROS generation, modulating the Nrf-2-antioxidant pathway, inhibiting MAPK signaling pathways, and decreasing NF-κB activation. Syr has been reported to protect UVA-induced skin photoaging by suppressing MMP-1 and pro-inflammatory cytokine production and increasing collagen in human keratinocytes and human fibroblasts via attenuating MAPK signaling pathways and their downstream activator protein 1 (AP-1), which is composed of c-Fos and c-Jun transcription activity [30]. However, the effects of Syr on UVB-induced skin damage have not been reported. As UVB radiation is more detrimental to the skin than UVA, this study aimed to investigate the protective effects of Syr on UVB-irradiated human dermal fibroblasts through its antioxidant and anti-inflammatory activities.

Materials and methods

Cell culture and maintenance

BJ human dermal fibroblasts (Lot No. 70015964, ATCC®-CRL-2522, USA) at the 5th to 15th passages were used in this study. The cells were maintained in Dulbecco's Modified Eagle Medium (DMEM) (Gibco, USA) supplemented with 10 % fetal bovine serum (Gibco, USA), 1 % penicillin, and streptomycin Gibco, USA) and incubated at 37 ºC with 5 % CO_2 in a humidified atmosphere. During use, the cells were subcultured using 0.25 % Trypsin-EDTA (Gibco, USA) twice weekly. Cells with more than 90 % viability were determined by 0.4 % trypan blue (Gibco, USA) staining at 1×10^5, 2×10^5, or 4×10^5 cells/mL were used in this study.

Syringaresinol

Syringaresinol, with >99.99 % purity at 254 nm, was isolated from stems and barks of *C. brachiata* collected in January 2018 from the botanical gardens of the Faculty of Pharmaceutical Sciences, Chulalongkorn University, Bangkok. The herbarium specimen was

deposited at the Department of Pharmacognosy and Pharmaceutical Botany, Chulalongkorn University. The handling and notification of stems and barks of *C. brachiata* were conducted according to the Plant Variety Protection Act B.E. 2542 (1999): Section 53, the Kingdom of Thailand. The isolation and characterization of Syr have been previously reported [21].

UVB-irradiation procedure and treatments

BJ cells were maintained in a fresh culture medium in a cell culture plate for 24 h, then washed twice with PBS and added 50 µL (in 96 well plates) or 500 µL (in 6 well plates) PBS to make a thin layer. The cells were irradiated using a UVB lamp (Philips 311 nm, TL 20W/01RS; Philips Lighting Holding BV (The Netherlands), positioned 12 cm above the plates with the total dose of UVB at 10 - 300 mJ/cm^2 (25 s - 12 min 30 s) determined by a UVB meter (Jedto Instruments, Thailand). The viability of irradiated cells was determined using a resazurin reduction assay to identify the maximum noncytotoxic and IC_{50} dose (UVB dose that causes 50 % cell inhibition from the maximal viability) for use in this study.

To evaluate the effects of Syr on irradiated cells, 3 defined concentrations of Syr were chosen based on its 2,2-diphenyl-1-picrylhydrazyl (DPPH) scavenging activity. BJ cells were maintained in fresh medium for 24 h and treated with Syr at 3, 10, and 30 µM or 100 µM vitamin C (Vit C) before irradiating with UVB radiation at the selected dose shown above. The irradiated cells were maintained at proper times before determining the parameters used to indicate the Syr activities. Untreated and non-irradiated BJ cells were used as the negative control in the study.

DPPH scavenging assay

The antioxidant activity of Syr was determined using a stable free radical DPPH scavenging assay. The final concentrations at 1 - 100 µM of Syr were used. A volume of 25 µL of Syr was mixed and reacted with 50 µL of 0.2 mM DPPH (Sigma-Aldrich, USA) for 30 min under light protection. The absorbances of the mixtures were determined at 520 nm using a microplate reader. Vitamin C (Vit C) and 0.2 % DMSO were used as the positive and solvent controls, respectively.

Resazurin reduction assay

The viability of BJ cells, when needed to be evaluated, was determined by resazurin reduction assay. The Syr or Vit C-treated and UVB-irradiated BJ cells were incubated with 50 µg/mL resazurin (Sigma-Aldrich, USA) for 4 h at 37 °C. The absorbance was measured at 560 and 600 nm. The viability of BJ cells was determined by comparing the percentage of viable cells with the solvent control.

2′,7′-Dichlorofluorescin diacetate (DCFDA) assay

Intracellular ROS levels were determined using 2′,7′-Dichlorofluorescin diacetate (DCFDA) (Sigma-Aldrich, USA). The treated and irradiated BJ cells were incubated with 30 µM DCFDA at 37 °C for 30 min, washed twice with PBS, and maintained in PBS. The fluorescence intensities were determined at 485 nm excitation and 535 nm emission using a fluorescence microplate reader. N-acetyl cysteine (NAC) at 5 mM was used as the positive control. UVB at the maximum noncytotoxic dose was used in this experiment.

Senescence-associated β-galactosidase (SA-β-gal) assay

To determine the protective effects of Syr on UVB-induced cellular senescence, the treated and irradiated BJ cells were maintained in a culture medium at 37 °C for 72 h before using a senescence β-galactosidase staining kit (Abcam, USA) to identify the senescent cells according to the manufacturing protocol. Briefly, the cells were washed once with phosphate buffered saline (PBS), fixed in 4 % paraformaldehyde for 10 min at room temperature, washed twice with PBS, and stained with a staining mixture solution (staining solution, staining supplement, and 20 mg/mL X-gal) at 37 °C for 24 h. Images were taken in at least 2 fields (100× magnification ~200 - 300 cells/field, at least 500 cells) for each well-plate using a light microscope (Nikon, USA). The number of SA-β-gal positive cells was counted using ImageJ software. The senescence rate was determined as the percentage of positive cells out of the cells. The maximum noncytotoxic dose of UVB was used in this experiment.

CPD-DNA assays

Cyclobutane pyrimidine dimer (CPD) levels in treated and irradiated BJ cells were determined after 1 h of irradiation according to the manufacturing protocol. Briefly, DNA was extracted from the cells using a NucleoSpin Tissue, a Mini kit for DNA from cells and tissue (Macherey-Nagel, Germany), and converted to single-strand DNA by incubating at 95 ºC for 10 min and then rapidly chilling on ice for 10 min. A volume of 50 µL of DNA at a concentration of 4 µg/mL was used to measure the CPD-DNA by using OxiSelect™ UV-Induced DNA Damage ELISA Kit (CPD Quantitation) (Cell Biolabs, Inc, USA) according to the manufacturing protocol. Briefly, DNA samples were mixed with a DNA-binding solution in a DNA-high binding plate for 24 h on an orbital shaker. The plates were washed twice with PBS and incubated with the assay solution for 1 h. The solution was then removed, and cells were incubated with 100 µL of anti-CPD antibody for 1 h on an orbital shaker, washed 5 times with washing buffer, and incubated with 100 µL secondary antibody-horseradish peroxidase (HRP) conjugate for 1 h. The supernatant was removed, and cells were washed 5 times with washing buffer and incubated with 100 µL substrate solution for 10 min, and the reaction was terminated with the stop solution. Finally, the absorbance at 450 nm was measured using a microplate reader. The maximum noncytotoxic dose of UVB at the maximum noncytotoxic dose was used in this experiment.

Enzyme-linked immunosorbent assay (ELISA)

Treated and irradiated BJ cells were incubated at 37 °C for 24 h. Culture supernatants were collected to determine the levels of TNF-α, IL-1, and IL-6 levels via enzyme-linked ELISA kits (human TNF-α, IL-1, IL-6) (Immuno Tools, Germany) according to the manufacturer's protocols. Briefly, plates were coated overnight with capture-antibody, removed the solution, blocked with a blocking buffer for 1 h at room temperature, incubated with the supernatants or the standard solutions for 2 h at room temperature, removed the solutions, washed, incubated with the detection antibodies for 2 h, washed and remove the solutions, incubated with poly-HRP-streptavidin for 30 min, incubated with TMB substrate for 10 min, added stop solution, and measured at 450 nm by using a microplate reader. The levels of TNF-α, IL-1, and IL-6 were calculated from the standard curve for each cytokine.

Western blot analysis

BJ cells were treated with Syr (3, 10, and 30 µM) or Vit C (100 µM) for 24 h, followed by UVB irradiation at 2 specific doses, depending on the targeted protein analysis. The treated cells were irradiated with UVB at its IC_{50} dose, 200 mJ/cm^2, to determine the proteins involved in apoptosis. After irradiation, cells were maintained in a fresh medium for 12 h before determining the levels of pro-caspase-3, cleaved caspase-3, PARP, and cleaved PARP using their specific antibodies, according to the company (Cell Signaling Technology, USA) recommendations with the following titers, anti-caspase-3 Ab (1:1000) and anti-PARP Ab (1:1000). For determining the levels of other proteins, treated cells were irradiated with UVB at a noncytotoxic dose, 40 mJ/cm^2, to avoid the confounding factor from cell death. After irradiation, cells were maintained in a fresh medium for the required time, according to previous studies, before protein levels were determined. The cells were maintained for 1 h before determining MAPKs, including ERK, JNK, p38, and their phosphorylated forms [31,32] using their specific antibodies, according to the company (Abcam, USA) recommendations with the following titers, anti-ERK Ab (1:2000), anti-pERK Ab (1:1000), anti-JNK Ab (1:1000), anti-pJNK Ab (1:1000), anti-p38 Ab (1:1000), and anti-p-p38 Ab (1:1000). Cells were maintained for 6 h before determining NF-κB with its specific Ab (1:1000) and Nrf2 with its specific Ab (1:1000), according to the company (Cell Signaling Technology, USA) recommendations. For the left of the proteins of interest, the cells were maintained for 24 h before the protein determination with their specific antibodies, according to the company recommendations, including anti-SOD Ab (1:1000), anti-CAT Ab (1:1000), anti-Col1A1 Ab (1:1000), and anti- p21 Ab (1:1000) from Cell Signaling Technology, USA; anti-HO-1 Ab (1:1000) from Abcam, USA; anti-MMP-1 Ab (1:1000) and anti-MMP-3 Ab (1:1000) from Elabscience Biotechnology Inc, USA. The timeline and experimental workflow are summarized in **Figure 1**.

Total proteins were isolated from cells using RIPA buffer (Abcam, USA) containing a protease and phosphatase inhibitor cocktail (Abcam, USA), and the protein contents were determined by using the bicinchoninic acid (BCA) method (Sigma-Aldrich, Germany). Nuclear and cytosolic proteins were isolated from cells using NE-PER™ nuclear and cytoplasmic extraction reagents (Thermo Scientific™, USA). For each sample, 20 µg of protein aliquots were run on 10 % SDS-PAGE gel and transferred to a nitrocellulose membrane. The membranes were blocked with 5 % nonfat dry milk in Tris-HCL-based buffered saline with 0.1 % Tween-20 (TBST blocking solution) for 1 h, washed with TBST 3 times for 5 min intervals, and incubated with the specific primary antibody against each protein of interest in the blocking solution overnight at 4 °C. Membranes were then washed 3 times with TBST for 5 min intervals before incubating with HRP-conjugated secondary antibody (Abcam, USA) in a blocking solution for 1 h. Immunoreactive bands were determined via the chemiluminescence method, and images were acquired using Image Studio software (LI-COR).

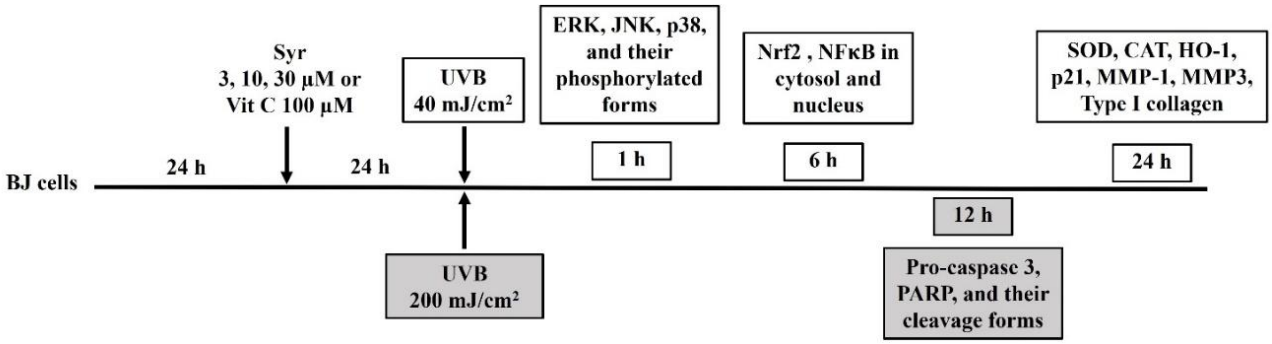

Figure 1 Determination of the proteins of interest by Western blot analysis. BJ cells were treated with Syr or Vitamin C for 24 h, irradiated with UVB at a noncytotoxic dose 40 mJ/cm^2 or at the IC_{50} dose 200 mJ/cm^2, maintained in a fresh culture medium at the different times for determining the level of each protein of interest; 1 h for the MAPK signaling molecules, 6 h for Nrf2 and NF-κB, 12 h for the apoptotic markers (caspase-3, PARP, and their cleavage forms), and 24 h for antioxidant enzymes, p21, MMPs, and collagen. The protein levels were compared to the UVB-irradiated control (n = 3).

Statistical analysis

Results from 3 independent experiments are presented as means and standard error of the means (mean ± SEM). Differences between test compounds and the suitable control were compared using the ANOVA (analysis of variance) test followed by Dunnett's post hoc test. SPSS version 22 was used for statistical analysis. A *p*-value of less than 0.05 was considered statistically significant.

Results and discussion

Syr demonstrated antioxidant activity at noncytotoxic concentrations in BJ cells

By using a DPPH scavenging assay, Syr exhibited potent antioxidant activity similar to that of Vit C, with their EC_{50} values at 16.90 ± 0.89 and 15.01 ± 0.81 µM, respectively (**Table 1**). The effect of Syr on BJ cell viability was determined by using the resazurin reduction assay. Syr and Vit C, at the concentrations of 3, 10, 30, 100, and 300 µM, had no effect on BJ cell viability (**Figure 2(A)**).

Table 1 DPPH scavenging activities of Syr and Vit C.

Compounds	EC_{50} (µM)
Vit C	15.01 ± 0.81
Syr	16.90 ± 0.89

Identification of UVB doses for this study

BJ cells were irradiated with UVB at 10 - 300 mJ/cm^2, then maintained in the culture medium for 24 h, and finally determined their viability by resazurin assay. The viability of the irradiated cells was significantly decreased when exposed to UVB at 50 - 300 mg/cm^2 with the maximum noncytotoxic dose at 40 mJ/cm^2, and an IC_{50} value was 203.93 mJ/cm^2 (**Figure 2(B)**). Therefore, UVB irradiation at 40 and 200 mJ/cm^2 was selected to evaluate the protective effects of Syr on irradiated BJ cells.

Syr decreased the ROS level in UVB-irradiated BJ cells

Within 30 min after UVB irradiation (40 mJ/cm^2), the intracellular ROS level in irradiated BJ cells was dramatically increased (2.5-fold) when compared with that in nonirradiated control. Syr at 10 and 30 µM and 100 µM Vit C significantly decreased the ROS level in the irradiated cells to 1.4-, 1.2-, and 1.2-fold, respectively (**Figure 2(C)**). NAC at 5 mM, the other well-known antioxidant, was also used as the positive control.

Syr reduced the senescence in UVB-irradiated BJ cells

When BJ cells were UVB-irradiated and maintained for 72 h in the culture medium, the number of senescence cells (43.01 ± 3.53 %) was significantly higher than that in the non-irradiated control (0.26 ± 0.02 %). Syr at 3, 10, and 30 µM significantly reduced the number of senescent cells to 24.70 ± 2.13, 16.91 ± 2.73, and 12.08 ± 1.56 %, respectively, and Vit C significantly decreased the senescent cells to 12.03 ± 1.22 % (**Figures 2(D)** and **2(E)**).

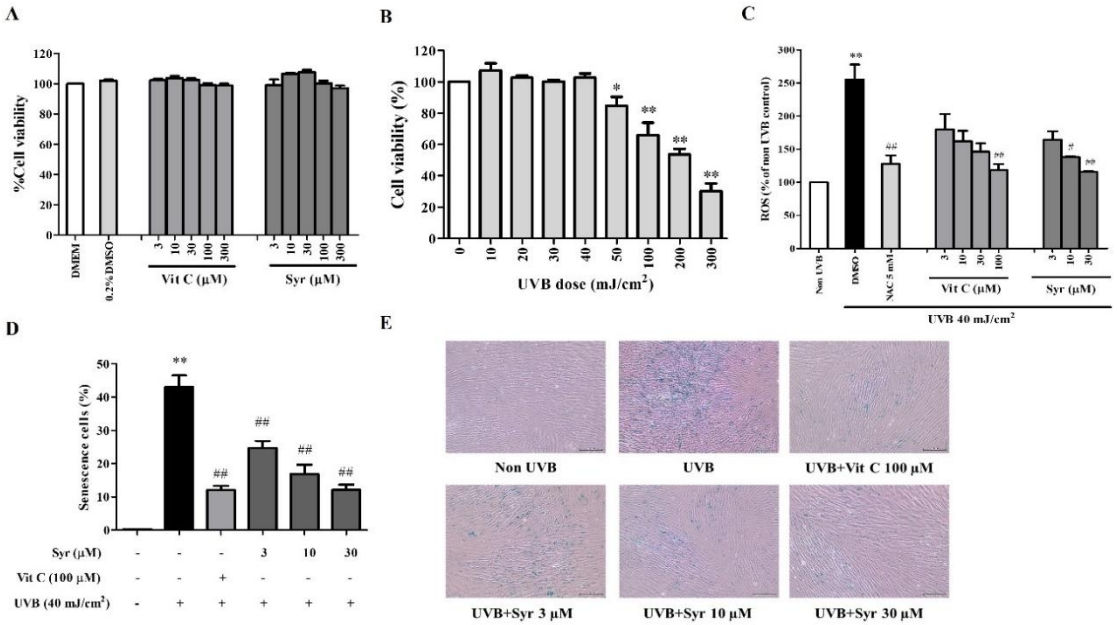

Figure 2 The effects of (A) Syr and (B) UVB radiation on the viability of BJ cells. Syr protected against (C) UVB-induced ROS generation and (D) UVB-induced increased percentage of senescent cells, which (E) representative figure of blue-stained senescent cells under a light microscope. $^{*}p < 0.05$, $^{**}p < 0.01$ compared to the non-irradiated control; $^{\#}p < 0.05$, $^{\#\#}p < 0.01$ compared to the UVB-irradiated control.

Syr improved the antioxidant system in UVB-irradiated BJ cells

Western blot analysis showed that UVB irradiation significantly decreased the levels of antioxidant enzymes, SOD (0.37 ± 0.01-fold), CAT (0.42 ± 0.02-fold), and HO-1 (0.44 ± 0.04-fold) in BJ cells. Syr at 3, 10 and 30 µM significantly increased the levels of SOD to 0.95 ± 0.22, 1.20 ± 0.19 and 1.49 ± 0.23-fold; the levels of CAT to 0.81 ± 0.02, 0.88 ± 0.01, and 1.16 ± 0.13-fold; and the levels of HO-1 to 1.52 ± 0.16, 1.81 ± 0.07, and 2.18 ± 0.21-fold of the non-irradiated control (**Figures 3(B) - (3D)**). Vit C at 100

μM also significantly reversed the effect of UVB by improving the levels of SOD, CAT, and HO-1 to 0.99 ± 0.11, 0.70 ± 0.06, and 1.27 ± 0.07-fold of the non-irradiated control, respectively (**Figures 3(B) - (3D)**).

The effect of Syr on Nrf2, an important transcription factor involved in upregulating the expression of several antioxidant proteins, was also evaluated. Syr at 30 μM increased the Nrf2 activity in the UVB-irradiated cells and significantly increased the level of nuclear NrF2 (3.87 ± 0.64-fold) (**Figure 3(F)**).

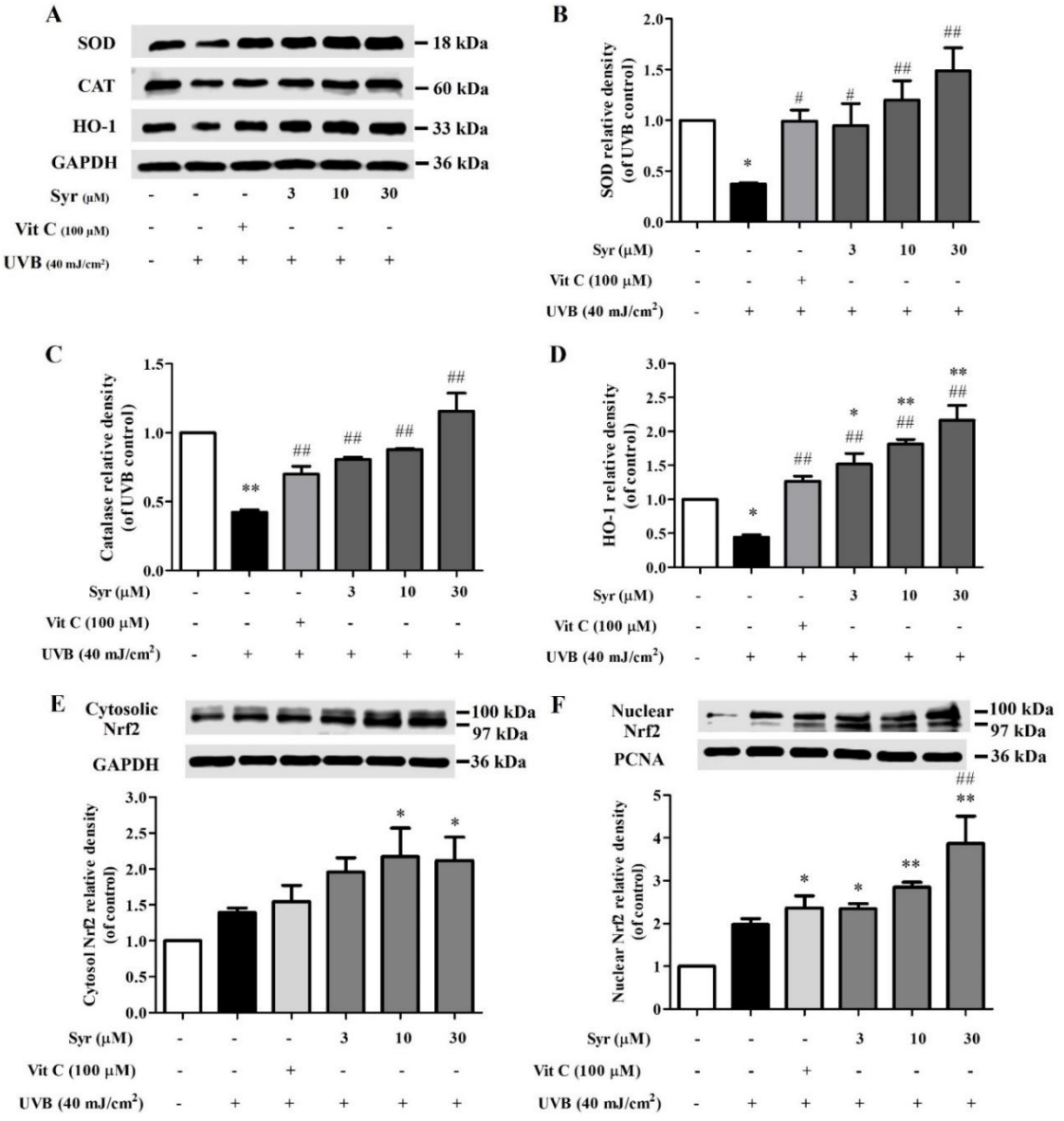

Figure 3 Effects of Syr on the levels of antioxidant enzymes and Nrf2 transcription factor. (A) Representative Western blots of antioxidant enzymes (SOD, CAT, and HO-1); (B) to (F): The levels of (B) SOD, (C) CAT, (D) HO-1, (E) cytosol Nrf2 and (F) nuclear Nrf2 are presented as the calculated densities relative to the non-irradiated control. $^{*}p < 0.05$, $^{**}p < 0.01$ compared to the non-irradiated control; $^{\#}p < 0.05$, $^{\#\#}p < 0.01$ compared to the UVB-irradiated control.

Syr decreased the amount of CPD photoproducts in UVB-irradiated BJ fibroblasts

CPD photoproducts were used as the markers of direct UVB-induced DNA damage. These products were not detected in non-irradiated BJ cells. However, 1 h after UVB irradiation, the levels of CPDs were significantly increased in UVB-irradiated BJ cells to 0.88 ± 0.05 ng/mL. Syr at 10 and 30 μM profoundly

protected cells from the effect of UVB-induced photoproducts by significantly deceased CPDs to 0.46 ± 0.09 and 0.08 ± 0.02 ng/mL, respectively. Syr at 3 µM and 100 µM Vit C did not affect the UVB-induced CPD generation (**Figure 4(A)**).

Syr prevented BJ cell senescence induced by UVB irradiation by modulating several molecules involved in senescence

Syr decreased p21 level

The results demonstrated the protective effect of Syr on UVB-induced p21 production. UVB dramatically increased the level of p21 in BJ cells to 5.17 ± 0.52-fold of the non-irradiated control (**Figure 4(B)**). Syr completely abolished this effect of UVB. Syr at 3, 10, and 30 µM significantly decreased the level of p21 to 1.53 ± 0.31, 1.09 ± 0.05, and 1.051.09 ± 0.08-fold of the non-irradiated control, respectively. Vit C at 100 µM significantly reduced the p21 level to 1.42 ± 0.21-fold (**Figure 4(B)**).

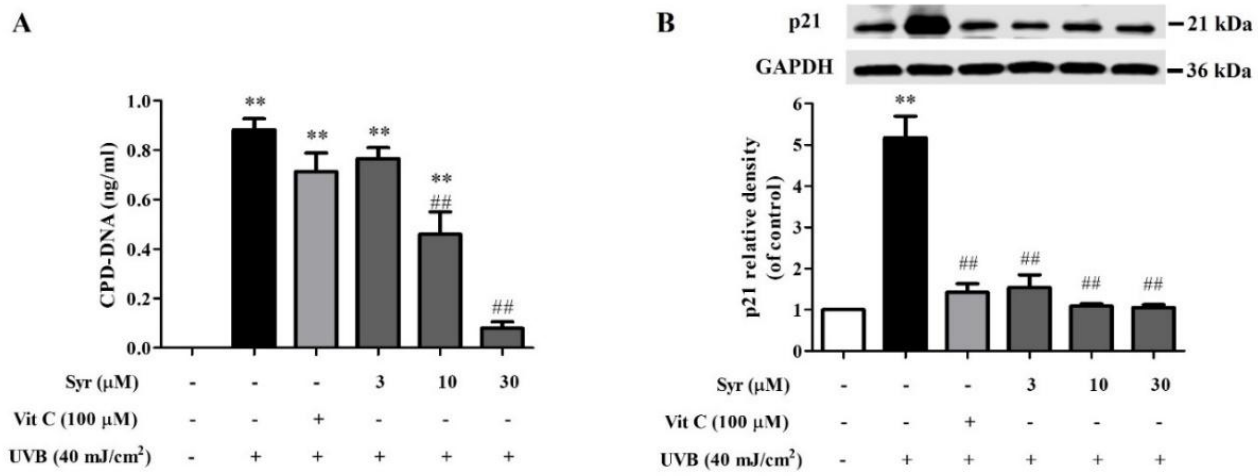

Figure 4 Effect of Syr on (A) direct UVB-induced DNA damage in irradiated BJ cells and (B) p21 level in UVB-irradiated BJ cells. $^{*}p < 0.05$, $^{**}p < 0.01$ compared to non-irradiated control; $^{\#}p < 0.05$, $^{\#\#}p < 0.01$ compared to UVB-irradiated control.

Syr decreased the levels of pro-inflammatory cytokines

UVB significantly increased the levels of pro-inflammatory cytokines; TNF-α (76.00 ± 7.73 pg/mL), IL-1β (132.04 ± 9.84 pg/mL), and IL-6 (176.63 ± 16.15 pg/mL), determined by ELISA at 24 h after irradiation. Syr significantly prevented these effects of UVB. In the irradiated BJ cells, Syr at 10 and 30 µM significantly reduced the levels of TNF-α to 52.11 ± 0.62 and 19.33 ± 2.83 pg/mL, IL-1β to 56.57 ± 9.82 and 13.98 ± 2.25 pg/mL, and IL-6 to 119.57 ± 16.13 and 89.13 ± 4.14 pg/mL, respectively. Syr at 30 µM completely inhibited the effect of UVB on these cytokines. The levels of these cytokines were almost similar to non-irradiated cells. Vit C at 100 µM significantly decreased the levels of TNF-α, IL-1β, and IL-6 to 41.00 ± 5.60, 35.28 ± 9.07, and 124.41 ± 6.46 pg/mL, respectively (**Figures 5(A) - 5(C)**).

Syr decreased MMP-1 and MMP-3 levels and increased type I collagen levels

UVB significantly increased the levels of MMP-1 (1.75 ± 0.17-fold) and MMP-3 (2.20 ± 0.10-fold) and decreased the level of collagen 1A1 (Col1A1) to 0.31 ± 0.06-fold of the non-irradiated control. Syr at all concentrations almost completely inhibited the effect of UVB on these enzymes. Syr at 3, 10, and 30 µM reduced the levels of MMP-1 to 1.45 ± 0.20, 1.13 ± 0.24, and 0.85 ± 0.04-fold of the non-irradiated cells, respectively, and decreased the levels of MMP-3 to 1.45 ± 0.20, 1.13 ± 0.24, and 0.85 ± 0.04-fold, respectively. Vit C had no effect on UVB-induced MMP production in BJ cells (**Figures 5(D)** and **5(E)**). Furthermore, Syr at 10 and 30 µM almost completely inhibited the effect of UVB on

CollA1 in irradiated BJ cells by increasing the levels of Col1A1 to 0.78 ± 0.07 and 1.06 ± 0.03-fold, respectively. The level of this protein was not different from the non-irradiated control (**Figure 5(F)**). Vit C at 100 µM did not modulate the effects of UVB on these proteins.

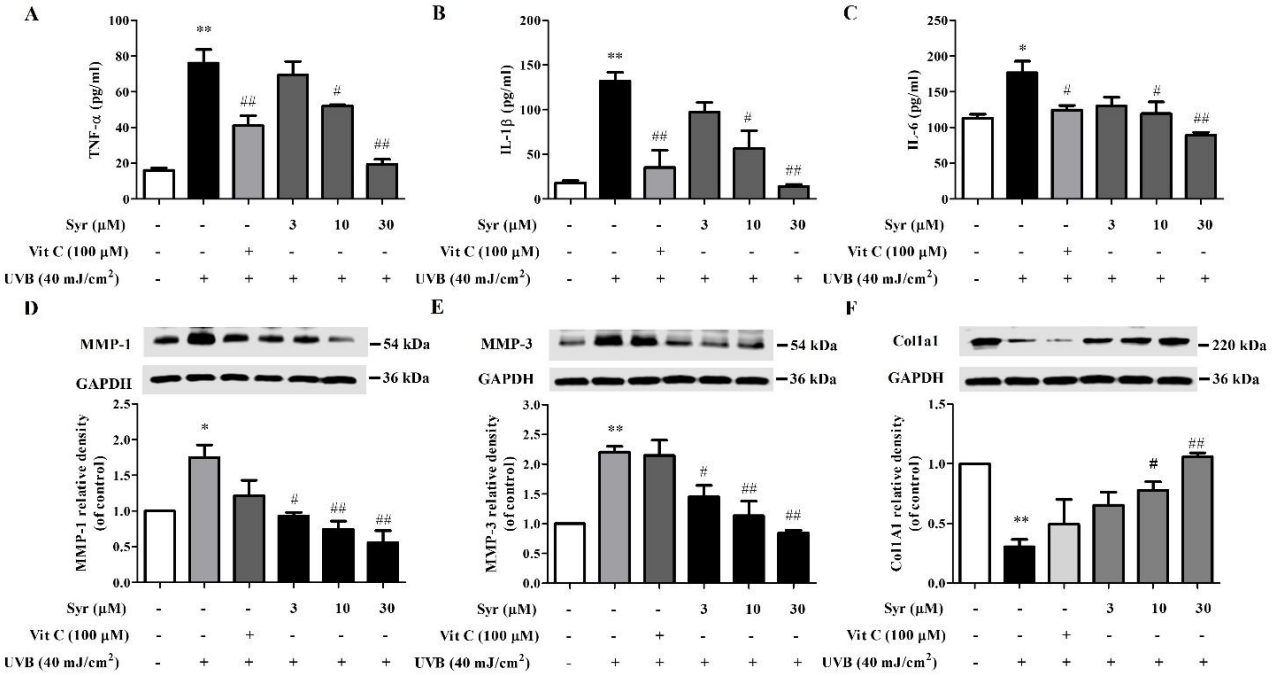

Figure 5 Effect of Syr on the levels of pro-inflammatory cytokines determining in the supernatants by ELISA; (A) TNF-α, (B) IL-1, and (C) IL-6, and the levels of (D) MMP-1, (E) MMP-3, and (F) Col1A1 determining the protein levels by Western blot analysis; in UVB-irradiated BJ cells. $^{*}p < 0.05$, $^{**}p < 0.01$ compared to the non-irradiated control; $^{\#}p < 0.05$, $^{\#\#}p < 0.01$ compared to the UVB-irradiated control.

Syr decreased the activated forms of MAPK signaling molecules and NF-κB induced by UVB in BJ cells

One h after UVB exposure, the levels of phosphorylated MAPKs, including phosphorylation of JNK (pJNK), p-38 (p-p38) and ERK (pERK) to 3.06 ± 0.52, 1.59 ± 0.03, 1.57 ± 0.19 -fold, respectively, when compared with that in non-irradiated control. Syr significantly inhibited these effects of UVB. In the irradiated BJ cells, Syr at 3, 10, and 30 µM significantly decreased the levels of pERK to 0.81 ± 0.15, 0.75 ± 0.18, 0.57 ± 0.09-fold of the non-irradiated control, respectively (**Figure 6(B)**), pJNK to 1.10 ± 0.35, 0.62 ± 0.18, and 0.61 ± 0.24 folds, respectively (**Figure 6(C)**). Syr at 30 µM significantly decreased the level of p-p38 to 0.76 ± 0.42 fold (**Figure 6(D)**), whereas Vit C at 100 µM did not affect p38 phosphorylation induced by UVB in BJ cells.

The effect of Syr on NF-κB activation was also investigated by determining the level of NF-κB in nuclei of UVB-irradiated cells. The level of nuclear NF-κB was significantly increased 6 h after UVB irradiation to 1.64 ± 0.05-fold of the non-irradiated control. Syr at 30 µM and Vit C at 100 µM significantly inhibited this effect by decreasing the nuclear levels of NFκB to 0.51 ± 0.10 and 0.68 ± 0.05-fold of the non-irradiated control, respectively, and the level of nuclear NF-κB was almost the same as that in the nonirradiated control (**Figure 6(F)**).

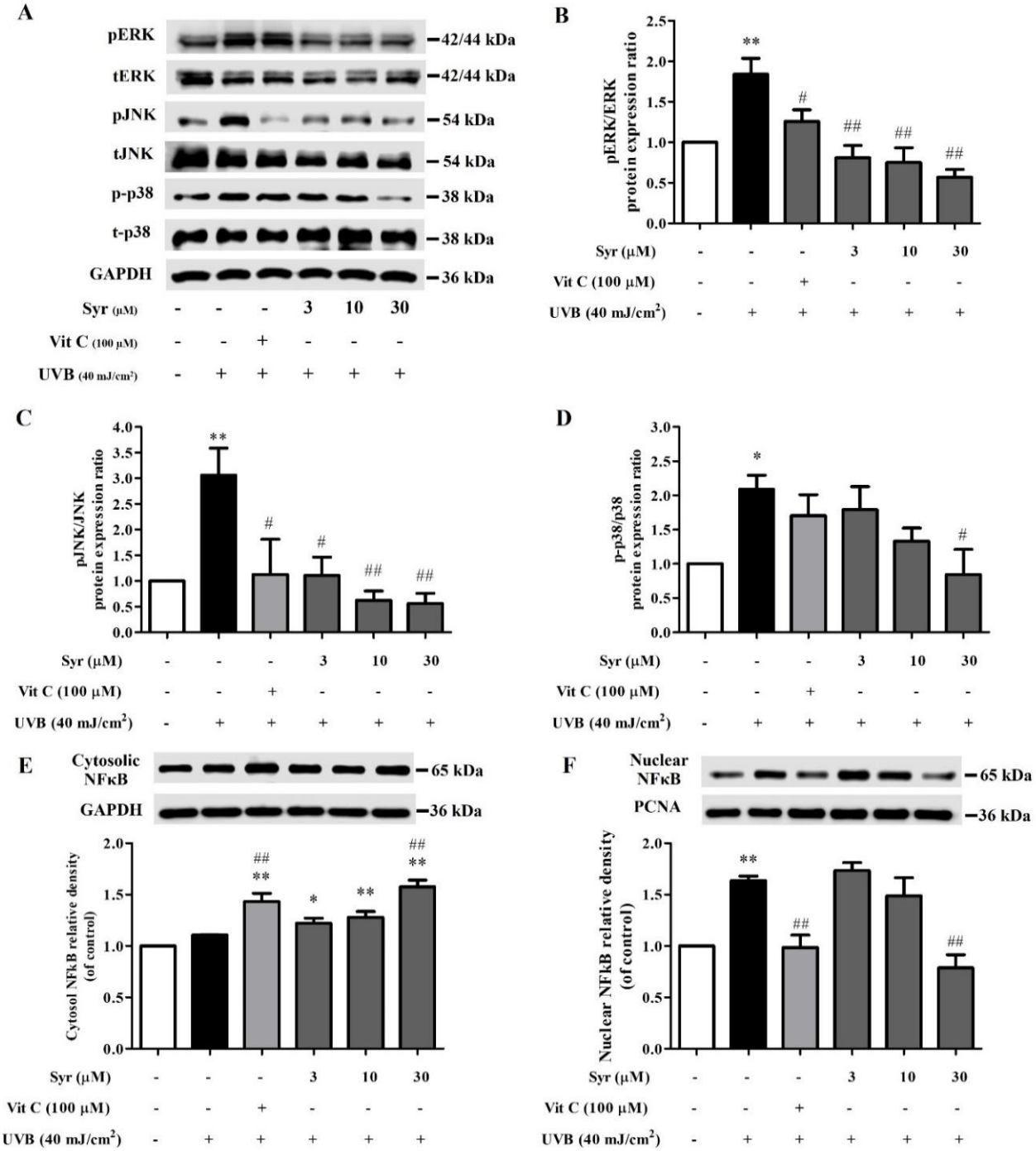

Figure 6 Effects of Syr on MAPK signaling pathways and NFκB activations in UVB-irradiated BJ cells. (A) Representative Western blots of MAPK signaling molecules (phosphorylated and total forms of ERK, JNK, and p38); B to D: The levels of phosphorylated and total forms of (B) ERK, (C) JNK, and (D) p38 are presented as the calculated densities relative to the non-irradiated control; E and F: The levels of (E) cytosolic NFκB and (F) nuclear NFκB. $^{*}p < 0.05$, $^{**}p < 0.01$ compared to the non-UVB control; $^{\#}p < 0.05$, $^{\#\#}p < 0.01$ compared to the UVB-irradiated control.

Syr protected BJ cells from UVB-induced apoptosis

UVB at its IC_{50} value, 200 mJ/cm^2, was used in this experiment. UVB decreased BJ cell viability after 24 h irradiation (51.43 ± 2.27 %) (**Figure 7(A)**). Cleaved caspase 3 and cleaved-PARP were used as the markers of apoptotic cells in this study. UVB significantly induced the generations of both cleaved-caspase 3 (5.77 ± 0.12-fold) and cleaved-PARP (2.73 ± 0.29-fold) (**Figures 7(B) - 7(D)**). Syr at 10 and 30 μM

significantly rescued BJ cells from the cytotoxic effect of UVB. It increased the viability of UVB-irradiated BJ cells to 69.15 ± 2.82 and 76.98 ± 2.03 %, respectively (**Figure 7(A)**). This protective effect of Syr was confirmed by the decrease of cleaved caspase 3 and cleaved-PARP levels in the irradiated cells (**Figures 7(B) - 7(D)**).

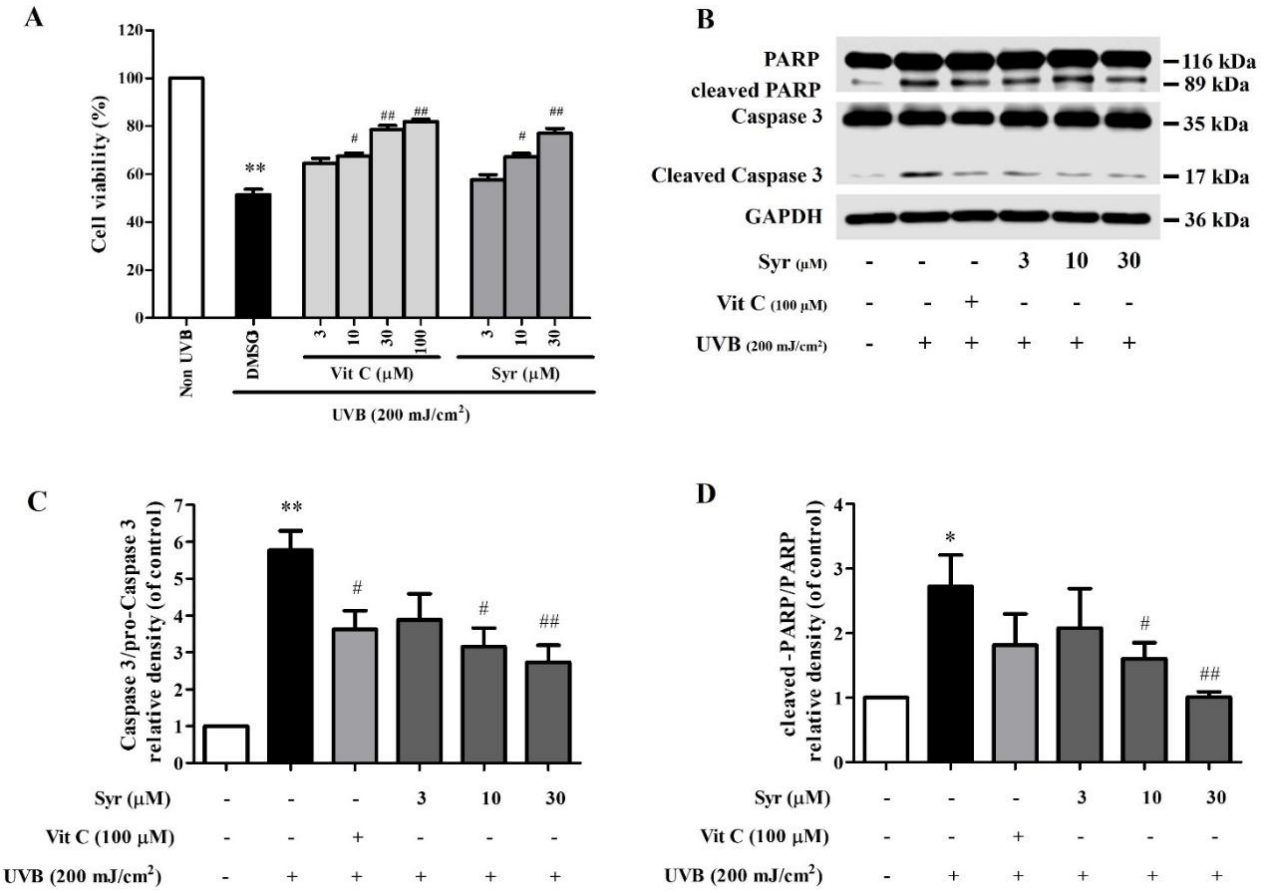

Figure 7 Effects of Syr on UVB-induced apoptosis of BJ cells by determining cell viability by resazurin assay and apoptotic markers by Western blot analysis; (A) percentage of BJ cell viability compared to the untreated and non-irradiated control. (B) Representative Western blots of apoptotic proteins, C and D: The levels of (C) pro-caspase 3 and cleaved caspase 3, and (D) PARP and its cleaved form are presented as the calculated densities relative to the non-irradiated control. $^{*}p < 0.05$, $^{**}p < 0.01$ compared to the non-irradiated control; $^{\#}p < 0.05$, $^{\#\#}p < 0.01$ compared to the UVB-irradiated control.

It has been documented that both UVA and UVB are factors that induce photoaging. It is well-documented that UV irradiation can cause intracellular oxidative stress by disrupting cellular redox homeostasis. It can induce intracellular ROS overproduction and decrease endogenous antioxidant capacities [32,33]. Oxidative distress state can compromise cellular homeostasis by causing genomic instability and DNA damage, protein degradation, membrane lipid abnormalities, and cellular dysfunction [33-35]. These detrimental effects can arrest the cell cycle, promote cell senescence, cause cell transformation, and induce cell death [36,37]. In this study, we identified the detrimental concentrations of the UVB radiation for human dermal fibroblasts and BJ cells and used these concentrations to evaluate its oxidative activities as well as to investigate the protective effects of Syr. We found that the IC_{50} and the maximum noncytotoxic concentrations of UVB radiation on BJ cells were 40 mJ/cm^2, and 203.93 mJ/cm^2, respectively. UVB at 40 mJ/cm^2 caused the imbalance of the cellular redox system in the irradiated

BJ cells. There was a profound increase in the ROS levels and a significant decrease in the levels of antioxidant enzymes, SOD, CAT, and HO-1, in the UVB-irradiated cells when compared to the non-irradiated cells. The accumulation of high levels of ROS mediates skin cell damage, leading to skin aging or photoaging and carcinogenesis [38,39]. Therefore, it is highly possible that agents with antioxidant capacities may protect against UVB-induced skin damage.

We used an *in vitro* DPPH-scavenging assay to demonstrate that Syr had potent antioxidant activity comparable to vitamin C, and effectively protects BJ cells from UVB-induced oxidative stress. We found that Syr scavenges ROS and significantly enhances antioxidant defenses by increasing levels of key enzymes (SOD, CAT, and HO-1) in irradiated cells. Syr also boosts Nrf2, the main regulator of antioxidant responses [40,41]. both in the cytosol and nucleus of UVB-exposed cells. This activation leads to the expression of antioxidant genes via the antioxidant response element (ARE) pathway, strengthening cellular defenses [42]. At physiological conditions, Nrf2 activity is negatively controlled by Kelch-like ECH-associated protein (Keap1) in the cytosol [43]. Keap1 binds cytosolic Nrf2 to facilitate constitutive Nrf2 degradation in the proteasome to maintain Nrf2 at the basal low level [44]. Upon oxidative stress, Keap1 is oxidized, undergoes conformation changes, and releases Nrf2. This causes Nrf2 stabilization and translocation to the nucleus to bind to the AREs and initiate the expression of antioxidant enzymes. Activation of Nrf2 has been shown to play a protective role in skin cells by inducing the expression of antioxidant enzymes in response to oxidative stress caused by environmental insults, including UV radiation. Enhancing Nrf2 activity can mitigate oxidative damage and improve skin cell resilience against ROS [42,43]. Accumulating evidence indicates that many natural compounds could partly improve skin photoaging by modulating Nrf2 activity [8]. Our findings suggest that Syr not only provides direct antioxidant effects by scavenging ROS but also via an indirect antioxidant activity by directly activating the Nrf2-ARE pathway, enhancing endogenous antioxidant production and restoring the redox balance in UVB-damaged fibroblasts.

UVB has been evidenced to cause DNA damage directly and indirectly via ROS in human skin cells. DNA directly absorbs UVB, which can induce UV-signature lesions, including cyclobutane pyrimidine dimers (CPDs) and pyrimidine (6-4) pyrimidone dimers (6-4PPs) [45]. These lesions are majority removed by DNA mechanisms. However, CPD photoproducts, the main lesions, are less efficiently repaired than 6-4PPs. UVB also indirectly causes oxidative DNA damage through its generated ROS, which induces DNA lesions, including 8-oxo-7,8-dihydro-2'-deoxyguanosine (8-oxodG) [6,46]. Depending on the UVB intensity and the duration of skin exposure, UVB-induced DNA lesions of skin cells can either undergo cell cycle arrest and apoptosis as a protective mechanism, resulting in cell cycle arrest and senescence, or skin cell transformation as harmful effects [20,47]. We found that UVB at the noncytotoxic dose (40 mJ/cm^2) generated CPD 6-4PPs within 1 h after exposure. Syr not only reduced UVB-induced oxidative stress in BJ cells, as mentioned above, but also impacted CPDs, the main biomarkers of direct UVB-induced DNA damage. Syr at 30 µM reduced the levels of CPD photoproducts in the UVB-irradiated BJ cells, whereas Vit C at 100 µM did not demonstrate any protective effects on the direct UVB damage on the DNA. These results suggest that Syr can alleviate both direct and indirect DNA damage induced by UVB.

We also demonstrated the protective effects of Syr on the consequences of DNA damage and oxidative stress induced by UVB at the noncytotoxic concentration in BJ cells. UVB-induced BJ senescence of more than 40 % within 72 h after irradiation when compared to the non-irradiated control. It also generated the senescence-associated secretory phenotype (SASP) in these irradiated cells by increasing the production of pro-inflammatory cytokines and MMPs, increasing the p21 level, and suppressing collagen synthesis. Syr could protect the irradiated cells from senescence by significantly reducing the number of SA-β-gal positive cells. Syr at 30 µM modulated the levels of all investigated senescent biomarkers to the basal levels of the non-irradiated cells. The compound significantly decreased the levels of pro-inflammatory cytokines, TNF-α, IL-1β, and IL-6, in the irradiated cells. UV radiation, oxidative stress, and pro-inflammatory cytokines are able to stimulate the production of MMPs, which contribute to skin photoaging by degrading extracellular matrix proteins such as collagen [48-50]. Syr could reduce the MMPs (MMP-1 and MMP-3)

levels in the irradiated BJ cells to their basal levels. Collagen is one of the principal supportive proteins for maintaining the elasticity and firmness of the skin. The decrease or decomposition of collagen results in skin wrinkles [51]. Col1A1 is decreased upon exposure to UV [52]. We found that UVB dramatically decreased the Col1A1 synthesis in UVB-irradiated BJ cells. Syr at 30 μM completely protected the effect of UVB on the Col1A1 synthesis. It also decreased the level of p21, which is involved in cell cycle arrest. Taken together, Syr seems to have protective effects on senescence induced by UVB exposure in BJ cells.

The cytotoxic effect of UVB interferes with normal skin functions and leads to skin cell damage and photoaging [53]. We investigated the effects of Syr on UVB-induced cell death. It has been reported that UVB induces apoptosis of dermal fibroblasts by causing DNA damage and by ROS [54,55]. These UVB-generated events trigger both the intrinsic and the extrinsic pathways of apoptosis and activate effector caspase 3 with the destruction of various caspase substrates as well as PARP, resulting in apoptosis [56,57]. When we exposed BJ cells to UVB at its IC_{50} dose concentration (200 mJ/cm^2), UVB increased pro-apoptotic markers, including cleaved caspase 3, cleaved PARP, and p21 levels. Syr increased cell survival and demonstrated an anti-apoptotic effect by decreasing all these markers in the irradiated cells. These results suggested that Syr is able to attenuate UVB-induced apoptotic cell death in human dermal fibroblasts. This pro-survival effect of Syr seems to be the consequence of the protective effects against oxidative stress and DNA damage of the compound.

The MAPK signaling pathways play crucial roles in UVB-induced skin damage [47,48] by activating ERK, JNK, and p38, which trigger transcription factors like AP-1 and NF-κB, leading to increased production of SASP-related cytokines and MMPs [56,57]. These pathways also modulated MAPK effector proteins, e.g., MK2 and MK5, which activate p53-independent DNA damage response (DDR) to promote cellular senescence [58,59]. It has been reported that antioxidants can counteract photoaging by blocking MAPK activation and reducing AP-1 and NF-κB activity [60,61]. In this study, Syr effectively inhibited the UVB-induced phosphorylation of ERK, JNK, and p38 MAPKs and suppressed NF-κB activity in the nucleus of irradiated BJ cells, suggesting it may also reduce AP-1 activity by inhibiting activated MAPKs to phosphorylate c-Fos and c-Jun, which are the components of AP-1. Syr has been reported to suppress UVA-induced inflammatory mediator and MMP-1 production in human dermal fibroblasts by targeting the MAPK signaling pathways, upstream activators of AP-1 activation and inflammatory response [30]. By targeting MAPK signaling, Syr reduced SASP factors and cellular senescence. These findings suggest that Syr may offer protective effects against both UVA- and UVB-induced skin damage, though further testing in human epidermal keratinocytes or skin models is recommended for broader application.

Conclusions

In conclusion, the results of this study reveal antioxidant and potential antiphotoaging properties of Syr at concentrations of 10 and 30 μM against UVB irradiation. Syr improved the balance of the oxidant-antioxidant system in UVB-irradiated human dermal fibroblasts. It had protective effects on cell survival and cellular senescence with SASP production, and collagen synthesizes against detrimental UVB effects. It is possible that the antioxidant activity of Syr plays an important part in reducing oxidative stress, which results in suppressing MAPK-mediated cellular senescence and apoptosis in the irradiated dermal fibroblasts.

Acknowledgments

This research was supported by the Ratchadapiseksompotch Fund, Faculty of Medicine, Chulalongkorn University, Grant number GA65/31, and Grant of Graduate School, Chulalongkorn University, Thailand.

The authors would like to thank the Department of Pharmacology, Faculty of Medicine, Chulalongkorn University, and Faculty of Integrative Medicine, Rajamangala University of Technology Thanyaburi, Thailand for facility support in this research. In addition, C. C. is supported by the Center of Excellence in Natural Products and Nanoparticles, CU.

References

[1] AV Nguyen and AM Soulika. The dynamics of the skin's immune system. *International Journal of Molecular Sciences* 2019; **20(8)**, 1811.

[2] C Parrado, S Mercado-Saenz, A Perez-Davo, Y Gilaberte, S Gonzalez and A Juarranz. Environmental stressors on skin aging. Mechanistic insights. *Frontiers in Pharmacology* 2019; **10**, 759.

[3] X Tang, T Yang, D Yu, H Xiong and S Zhang. Current insights and future perspectives of ultraviolet radiation (UV) exposure: Friends and foes to the skin and beyond the skin. *Environment International* 2024; **185**, 108535.

[4] M Wei, X He, N Liu and H Deng. Role of reactive oxygen species in ultraviolet-induced photodamage of the skin. *Cell Division* 2024; **19(1)**, 1.

[5] T Al-Sadek and N Yusuf. Ultraviolet radiation biological and medical implications. *Current Issues in Molecular Biology* 2024; **46**, 1924-1942.

[6] AP Schuch, NC Moreno, NJ Schuch, CFM Menck and CCM Garcia. Sunlight damage to cellular DNA: Focus on oxidatively generated lesions. *Free Radical Biology and Medicine* 2017; **107**, 110-124.

[7] J Cadet, T Douki and JL Ravanat. Oxidatively generated damage to cellular DNA by UVB and UVA radiation. *Photochemistry and Photobiology* 2015; **91(1)**, 140-155.

[8] D Mohania, S Chandel, P Kumar, V Verma, K Digvijay, D Tripathi, K Choudhury, SK Mitten and D Shah. Ultraviolet radiations: Skin defense-damage mechanism. *Advances in Experimental Medicine and Biology* 2017; **996**, 71-87.

[9] U Panich, G Sittithumcharee, N Rathviboon and S Jirawatnotai. Ultraviolet radiation-induced skin aging: The role of DNA damage and oxidative stress in epidermal stem cell damage mediated skin aging. *Stem Cells International* 2016; **2016**, 7370642.

[10] C Espinosa-Diez, V Miguel, D Mennerich, T Kietzmann, P Sanchez-Perez, S Cadenas and S Lamas. Antioxidant responses and cellular adjustments to oxidative stress. *Redox Biology* 2015; **6**, 183-197.

[11] TM Ansary, MR Hossain, K Kamiya, M Komine and M Ohtsuki. Inflammatory molecules associated with ultraviolet radiation-mediated skin aging. *International Journal of Molecular Sciences* 2021; **22(8)**, 3974.

[12] J Zhang, X Wang, V Vikash, Q Ye, D Wu, Y Liu and W Dong. ROS and ROS-mediated cellular signaling. *Oxidative Medicine and Cellular Longevity* 2016; **2016**, 4350965.

[13] C Anerillas, K Abdelmohsen and M Gorospe. Regulation of senescence traits by MAPKs. *GeroScience* 2020; **42**, 397-408.

[14] A Gegotek and E Skrzydlewska. The role of transcription factor Nrf2 in skin cells metabolism. *Archives of Dermatological Research* 2015; **307(5)**, 385-396.

[15] JA Zhang, C Luan, D Huang, M Ju, K Chen and H Gu. Induction of autophagy by baicalin through the AMPK-mTOR pathway protects human skin fibroblasts from ultraviolet B radiation-induced apoptosis. *Drug Design, Development and Therapy* 2020; **14**, 417-428.

[16] W Choi, HS Kim, SH Park, D Kim, YD Hong, JH Kim and JY Cho. Syringaresinol derived from *Panax ginseng* berry attenuates oxidative stress-induced skin aging via autophagy. *Journal of Ginseng Research* 2022; **46(4)**, 536-542.

[17] YS Cho, WS Song, SH Yoon, KY Park and MH Kim. Syringaresinol suppresses excitatory synaptic transmission and picrotoxin-induced epileptic activity in the hippocampus through presynaptic mechanisms. *Neuropharmacology* 2018; **131**, 68-82.

[18] W Monthong, S Pitchuanchom, N Nuntasaen and W Pompimon. (+)-Syringaresinol lignan from new species *Magnolia Thailandica*. *American Journal of Applied Sciences* 2011; **8(12)**, 1268-1271.

[19] VK Bajpai, MB Alam, KT Quan, MK Ju, R Majumder, S Shukla, YS Huh, M Na, SH Lee and YK Han. Attenuation of inflammatory responses by (+)-syringaresinol via MAP-Kinase-mediated suppression of NF-κB signaling *in vitro* and *in vivo*. *Scientific Reports* 2018; **8(1)**, 9216.

[20] Y Lin, S Li, T Chen, Y Lin, Z Cheng, L Ni, JJ Lu and M Huang. Phytochemical compositions and biological activities of the branches and leaves of *Ormosia hosiei* Hemsl. et Wils. *Journal of Pharmaceutical and Biomedical Analysis* 2023; **226**, 115238.

[21] N Nalinratana, U Suriya, C Laprasert, N Wisidsri, P Poldorn, T Rungrotmongkol, W

Limpanasitthikul, HC Wu, HS Chang and C Chansriniyom. *In vitro* and *in silico* studies of 7″,8″-buddlenol D anti-inflammatory lignans from *Carallia brachiata* as p38 MAP kinase inhibitors. *Scientific Reports* 2023; **13(1)**, 3558.

[22] G Li, C Liu, L Yang, L Feng, S Zhang, J An, J Li, Y Gao, Z Pan, Y Xu, J Liu, Y Wang, J Yan, J Cui, Z Qi and L Yang. Syringaresinol protects against diabetic nephropathy by inhibiting pyroptosis via NRF2-mediated antioxidant pathway. *Cell Biology and Toxicology* 2023; **39(3)**, 621-639.

[23] BY Park, SR Oh, KS Ahn, OK Kwon and HK Lee. (-)-Syringaresinol inhibits proliferation of human promyelocytic HL-60 leukemia cells via G1 arres and apoptosis. *International Immunopharmacology* 2008; **8(7)**, 967-973.

[24] L Zhang, X Jiang, J Zhang, H Gao, L Yang, D Li, Q Zhang, B Wang, L Cui and X Wang. (-)-Syringaresinol suppressed LPS-induced microglia activation via downregulation of NF-κB p65 signaling and interaction with ERβ. *International Immunopharmacology* 2021; **99**, 107986.

[25] X Wang, D Wang, B Deng and L Yan. Syringaresinol attenuates osteoarthritis via regulating the NF-κB pathway. *International Immunopharmacology* 2023; **118**, 109982.

[26] S Cho, M Cho, J Kim, M Kaeberlein, SJ Lee and Y Suh. Syringaresinol protects against hypoxia/reoxygenation-induced cardiomyocytes injury and death by destabilization of HIF-1α in a FOXO3-dependent mechanism. *Oncotarget* 2015; **6(1)**, 43-55.

[27] A Wei, J Liu, D Li, Y Lu, L Yang, Y Zhuo, W Tian and H Cong. Syringaresinol attenuates sepsis-induced cardiac dysfunction by inhibiting inflammation and pyroptosis in mice. *European Journal of Pharmacology* 2021; **913**, 174644.

[28] M Miyazawa, H Utsunomiya, K Inada, T Yamada, Y Okuno, H Tanaka and M Tatematsu. Inhibition of *Helicobacter pylori* motility by (+)-Syringaresinol from unripe *Japanese apricot*. *Biological & Pharmceutical Bulletin* 2006; **29(1)**, 172-173.

[29] J Kim, T Toda, K Watanabe, S Shibuya, Y Ozawa, N Izuo, S Cho, DB Seo, K Yokote and T Shimizu. Syringaresinol reverses age-related skin atrophy by suppressing FoxO3a-mediated matrix metalloproteinase-2 activation in copper/zinc superoxide dismutase-deficient dice. *Journal of Investigative Dermatology* 2019; **139(3)**, 648-655.

[30] JH Oh, YH Joo, F Karadeniz, J Ko and CS Kong. Syringaresinol inhibits UVA-induced MMP-1 expression by suppression of MAPK/AP-1 signaling in HaCaT keratinocytes and human dermal fibroblasts. *International Journal of Molecular Sciences* 2020; **21(11**), 3981.

[31] AP Schuch, NC Moreno, NJ Schuch, CFM Menck and CCM Garcia. Sunlight damage to cellular DNA: Focus on oxidatively generated lesions. *Free Radical Biology & Medicine* 2017; **107**, 110-124.

[32] H Masaki. Role of antioxidants in the skin: Anti-aging effects. *Journal of Dermatological Science* 2010; **58(2)**, 85-90.

[33] E Markiewicz and OC Idowu. DNA damage in human skin and the capacities of natural compounds to modulate the bystander signalling. *Open Biology* 2019; **9(12)**, 190208.

[34] Y Xu and GJ Fisher. Ultraviolet (UV) light irradiation induced signal transduction in skin photoaging. *Journal of Dermatological Science Supplement* 2005; **1(2)**, S1-S8.

[35] R Pandel, B Poljšak, A Godic and R Dahmane. Skin photoaging and the role of antioxidants in its prevention. *ISRN Dermatology* 2013; **2013**, 930164.

[36] O Tavana, CL Benjamin, N Puebla-Osorio, M Sang, SE Ullrich, HN Ananthaswamy and C Zhu. Absence of p53-dependent apoptosis leads to UV radiation hypersensitivity, enhanced immunosuppression and cellular senescence. *Cell Cycle* 2010; **9(16)**, 3328-3336.

[37] Y Sha, V Vartanian, N Owen, SJM Koon, MJ Calkins, CS Thompson, Z Mirafzali, S Mir, LE Goldsmith, H He, C Luo, SM Brown, PW Doetsch, A Kaempf, JY Lim, AK McCullough and RS Lloyd. Modulation of UVB-induced carcinogenesis by activation of alternative DNA repair pathways. *Scientific Reports* 2018; **8(1)**, 705.

[38] F Bonté, D Girard, JC Archambault and A Desmouliere. Skin changes during ageing. *Sub-cellular Biochemistry* 2019; **91**, 249-280.

[39] M Furue, H Uchi, C Mitoma, A Hashimoto-Hachiya, T Chiba, T Ito, T Nakahara and G Tsuji. Antioxidants for healthy skin: The emerging role of aryl hydrocarbon receptors and nuclear factor-erythroid 2-related factor-2. *Nutrients* 2017; **9(3)**, 223.

[40] C Yu and JH Xiao. The Keap1-Nrf2 system: A mediator between oxidative stress and aging. *Oxidative Medicine and Cellular Longevity* 2021; **2021**, 6635460.

[41] L Baird and M Yamamoto. The molecular mechanisms regulating the KEAP1-NRF2 pathway. *Molecular and Cellular Biology* 2020; **40(13)**, e00099-20.

[42] RA Zinovkin, ND Kondratenko and LA Zinovkina. Does Nrf2 play a role of a master regulator of mammalian aging? *Biochemistry* 2022; **87(12**), 1465-1476.

[43] D Xian, X Xiong, J Xu, L Xian, Q Lei, J Song and J Zhong. Nrf2 overexpression for the protective effect of skin-derived precursors against UV-induced damage: Evidence from a three-dimensional skin model. *Oxidative Medicine and Cellular Longevity* 2019; **2019**, 7021428.

[44] YC Boo. Natural Nrf2 modulators for skin protection. *Antioxidants* 2020; **9(9)**, 812.

[45] T Budden and NA Bowden. The role of altered nucleotide excision repair and UVB-induced DNA damage in melanomagenesis. *International Journey of Molecular Sciences* 2013; **14(1)**, 1132-1151.

[46] M Mijit, V Caracciolo, A Melillo, F Amicarelli and A Giordano. Role of p53 in the regulation of cellular senescence. *Biomolecules* 2020; **10(3)**, 420.

[47] BG Childs, DJ Baker, JL Kirkland, J Campisi and JMV Deursen. Senescence and apoptosis: Dueling or complementary cell fates? *EMBO Reports* 2014; **15**, 1139-1153.

[48] SI Choi, JH Lee, JM Kim, TD Jung, BY Cho, SH Choi, DW Lee, J Kim, JY Kim and OH Lee. *Ulmus macrocarpa* hance extracts attenuated H_2O_2 and UVB-induced skin photo-aging by activating antioxidant enzymes and inhibiting MAPK pathways. *International Journal Molecular Sciences* 2017; **18(6)**, 1200.

[49] HS Han, JS Shin, DB Myung, HS Ahn, SH Lee, HJ Kim and KT Lee. *Hydrangea serrata* (Thunb.) Ser. extract attenuate UVB-induced photoaging through MAPK/AP-1 inactivation in human skin fibroblasts and hairless mice. *Nutrients* 2019; **11(3)**, 533.

[50] JP Kumar and BB Mandal. Inhibitory role of silk cocoon extract against elastase, hyaluronidase and UV radiation-induced matrix metalloproteinase expression in human dermal fibroblasts and keratinocytes. *Photochemical & Photobiological Sciences* 2019; **18(5)**, 1259-1274.

[51] JW Shin, SH Kwon, JY Choi, JI Na, CH Huh, HR Choi and KC Park. Molecular mechanisms of dermal aging and antiaging approaches. *International Journal of Molecular Sciences* 2019; **20(9)**, 2126.

[52] C Marionnet, C Pierrard, F Lejeune and F Bernerd. Modulations of gene expression induced by daily ultraviolet light can be prevented by a broad spectrum sunscreen. *Journal of Photochemistry and Photobiology B: Biology* 2012; **116**, 37-47.

[53] SW Shin, E Jung, S Kim, JH Kim, EG Kim, J Lee and D Park. Antagonizing effects and mechanisms of afzelin against UVB-induced cell damage. *PLoS One* 2013; **8(4)**, e61971.

[54] M Deng, D Li, Y Zhang, G Zhou, W Liu, Y Cao and W Zhang. Protective effect of crocin on ultraviolet B-induced dermal fibroblast photoaging. *Molecular Medicine Reports* 2018; **18**, 1439-1446.

[55] E Mavrogonatou, M Angelopoulou, SV Rizou, H Pratsinis, VG Gorgoulis and D Kletsas. Activation of the JNKs/ATM-p53 axis is indispensable for the cytoprotection of dermal fibroblasts exposed to UVB radiation. *Cell Death & Disease* 2022; **13(7)**, 647.

[56] AS Gary and PJ Rochette. Apoptosis, the only cell death pathway that can be measured in human diploid dermal fibroblasts following lethal UVB irradiation. *Scientific Reports* 2020; **10(1)**, 18946.

[57] AB Parrish, CD Freel and S Kornbluth. Cellular mechanisms controlling caspase activation and function. *Cold Spring Harbor Perspective in Biology* 2013; **5(6)**, a008672.

[58] HJ Choi, MB Alam, ME Baek, YG Kwon, JY Lim and SH Lee. Protection against UVB-induced

photoaging by *Nypa fruticans* via inhibition of MAPK/AP-1/MMP-1 signaling. *Oxidative Medicine and Cellular Longevity* 2020; **2020**, 2905362.

[59] V Muthusamy and TJ Piva. The UV response of the skin: A review of the MAPK, NFκB and TNFα signal transduction pathways. *Archives of Dermatological Research* 2010; **302(1)**, 5-17.

[60] T Shi and TB Dansen. Reactive oxygen species induced p53 activation: DNA damage, redox signaling, or both? *Antioxidants & Redox Signaling* 2020; **33(12)**, 839-859.

[61] S Dunaway, R Odin, L Zhou, L Ji, Y Zhang and AL Kadekaro. Natural antioxidants: Multiple mechanisms to protect skin from solar radiation. *Frontiers Pharmacology* 2018; **9**, 392.